Low-temperature magnetoresistance effect and thermoelectric properties of polycrystalline $FeAs_2$ thin film on $LaAlO_3$ (100) substrate

Hiệu ứng từ điện trở nhiệt độ thấp và tính chất nhiệt điện của màng mỏng đa tinh thể $FeAs_2$ trên đế $LaAlO_3$ (100)

Duong Van Thiet[1,*], Nguyen Xuan Chung[2], Nguyen Tien Tung[2], Nguyen Quoc Tuan[1], Nguyen Minh Quang[1], Sunglae Cho[3,*]

[1]*Faculty of Mechanical Engineering, Hanoi University of Industry*

[2]*Department of Physics, Hanoi University of Mining and Geology*

[3]*Department of physics, University of Ulsan, Republic of Korea*

[*]*Email: dvthiet86@haui.edu.vn*

Keywords:

$FeAs_2$, MBE, magnetoresistance, thermoelectric, thin film

Abstract

The polycrystalline $FeAs_2$ thin film grown on a $LaAlO_3$ (100) substrate by using molecular beam epitaxy (MBE) has been investigated. The origin of negative magnetoresistance (MR) is observed at 20K due to hopping conduction mechanism. The films exhibit semiconductor behavior with dominant charge-carrier being electron. Above room temperature, the electrical activation energy is estimated to be 0.20*eV*, that original from transport mechanism such as thermionic emission. The maximal Seebeck coefficient is, S = -138μV/K at T = 300K.

Từ khóa:

$FeAs_2$, MBE, từ điện trở, nhiệt điện, màng mỏng

Tóm tắt

Trong báo cáo này chúng tôi báo cáo vào tính chất của màng mỏng $FeAs_2$ đa tinh thể lắng đọng trên đế $LaAlO_3$ (100) sử dụng hệ bốc bay chùm phân tử (MBE). Nguồn gốc hiệu ứng từ điện trở âm được quan sát tại nhiệt độ 20K có thể do cơ chế dẫn hopping. Màng mỏng thể hiện tính chất bán dẫn với hạt tải điện là điện tử. Trong khoảng nhiệt trên độ phòng năng lượng hoạt hóa của màng mỏng là 0,20*eV.* Nguồn gốc cơ chế dẫn trong khoảng nhiệt độ này đạt được là do hiệu ứng phát xạ nhiệt. Hệ số Seebeck lớn nhất đạt được trong màng mỏng này là -138μV/K tại nhiệt độ 300K.

1. INTRODUCTION

Nowadays, using thermoelectric materials to convert thermal energies into electric energy and vice versa is a promising technique but it is still limited [1]. To evaluate efficiency of these materials, the thermoelectric dimensionless figure of merit $ZT = S^2T/\rho\kappa$ is often used, where S is the Seebeck coefficient, ρ is electrical resistivity, κ is thermal conductivity, and T is temperature [2]. The high value of ZT is achieved by either increasing S^2/ρ (called power factor) or reduction of κ.

$FeAs_2$ is also known as a candidate material with high Seebeck coefficient on both theory and experiment [3-7]. It is a semiconductor with bandgap of 0.22 eV, the crystal structure is orthorhombic Marcasite (space group *Pnm*) with the lattice parameters; a = 5.299, b = 5.984, and c = 2.882 Å. The iron atom is coordinated by six arsenic atoms forming distorted $FeAs_6$-octahedral that share corners along the c axis. Each anion is coordinated by three irons and another arsenic atom forming distorted tetrahedral site [3]. The peculiar band gap structure of $FeAs_2$ makes its unique thermoelectric properties [3-6]. In the early 1970s, Fan *et al.* reported the thermoelectric property of single crystal of $FeAs_2$ with Seebeck coefficient at room temperature approximately -200μV/K [3]. A huge Seebeck coefficient of -7 mV/K is obtained at the temperature of 12K [4-5]. Recently, Usui *et al.* shown that *electron-doped* polycrystalline $FeAs_2$ exhibits metallic with a large Seebeck coefficient at 300 K, about -200 μV/K, for 1% selenium doping driven by quasi-one-dimensional pudding-mod-type band [6-7]. However, the details of electrical conduction mechanism of polycrystalline $FeAs_2$ film, and magnetoresistance effect at low temperature are not still reported.

In this paper, we report on structural, transport and thermoelectric properties of polycrystalline $FeAs_2$ thin film grown on $LaAlO_3$ (100) substrate using molecular beam epitaxy (MBE). The film shows a negative magnetoresistance at the temperature of 20K. The maximal Seebeck coefficient of -138 μV/K is investigated around room temperature.

2. METHODS

A $FeAs_2$ film was grown on a (100) $LaAlO_3$ substrate by using MBE system (VG Semicon, Inc.). The substrate was chemically cleaned before loading the substrate into the growth chamber. The substrate was heated up to 700 °C for 30 min to completely remove the residual impurities. The substrate was cooled down and stabilized at growth temperature of 300 °C. The evaporation rate of Fe was 0.26 Å/s, and the As pressure was 1.8×10^{-6} Torr during the growth. For Fe evaporation, we used a high temperature effusion cell and for As, we used the As cracking cell. The evaporation rate was confirmed by quartz crystal microbalance and ion gauge beam flux monitor. The growth quality, we used reflection high - energy electron diffraction (RHEED) for the *in-situ* observation of crystal structure and surface morphology. The crystal structures of the samples were characterized by X-ray diffraction (XRD). The surface morphology and roughness of $FeAs_2$ film were characterized by field emission scan electron

microscopy (FE-SEM). The crystal structure of the sample was characterized by X-ray diffraction (XRD) investigation. The electrical resistivity was measured by using a four-probe van der Pauw configuration. The differential method was used to determine the Seebeck coefficient, where thermoelectric voltage was measured by maintaining small temperature difference constant across the sample by employing $\Delta V = S\nabla T$ and ignoring higher order ∇T terms. The Seebeck coefficient is determined from the slope in linear region of ΔV_i versus ∇T_i.

3. RESULTS AND DISCUSSION

3.1. The morphology of $FeAs_2$ film on (100) $LaAlO_3$ substrate

The ratio of Fe and As concentrations determined from electron probe microanalyzer (EPMA) measurement system is 1:2. Fig. 1(a) shows ring-shape RHEED pattern, a characterization was polycrystalline of $FeAs_2$ film. Fig. 1(b) shows the secondary electron image (SEI) characterized by arrangement of like-particles with the root mean square (RMS) of 4.33 nm. Furthermore, the compositional image produced by backscattered electron (BEI-COMPO) indicates homology surface, and an evident of no cluster is e found as shown in Fig. 1 (c). The inset in Fig. 1 (b) is the cross-section SEM image, indicating the layer thickness approximately 100 nm.

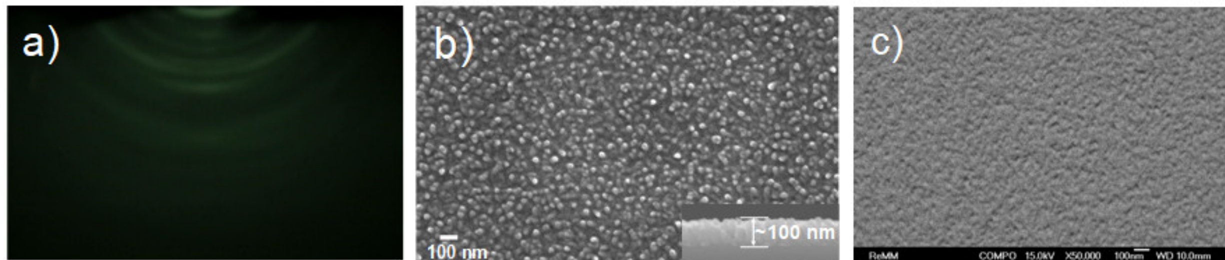

Fig. 1. RHEED patterns (a), SEM (b) and COMPO (c) images of the $FeAs_2$ film on (100) $LaAlO_3$ substrate using MBE. The inset in Fig. 1 (b) shows the cross-section.

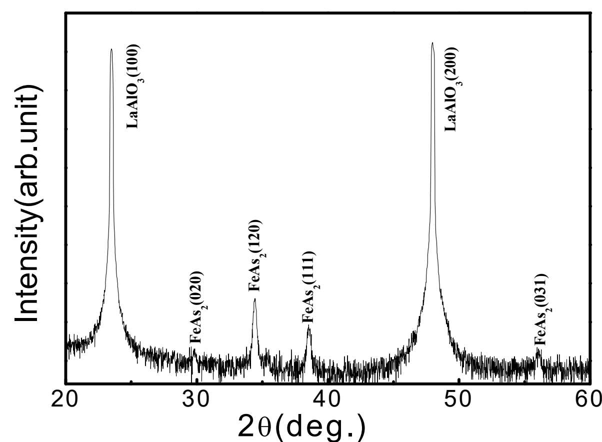

Fig. 2. The θ-2θ X-ray diffraction patterns of the $FeAs_2$ films on $LaAlO_3$ substrate

The crystal structure of $FeAs_2$ thin film was investigated by using XRD measurements, as shown in Fig. 2. There are four distinct peaks at 29.82, 34.42, 38.54, and 56.05°, which indexed (020), (120), (111), and (031), respectively. All XRD patterns can be indexed to a pure orthorhombic phase consistent with the reported data (JCPDS: 79-0251). The result shows that the film is polycrystallinewith the lattice constants a = 5.276 Å, b = 5.991 Å and c = 2.892 Å.

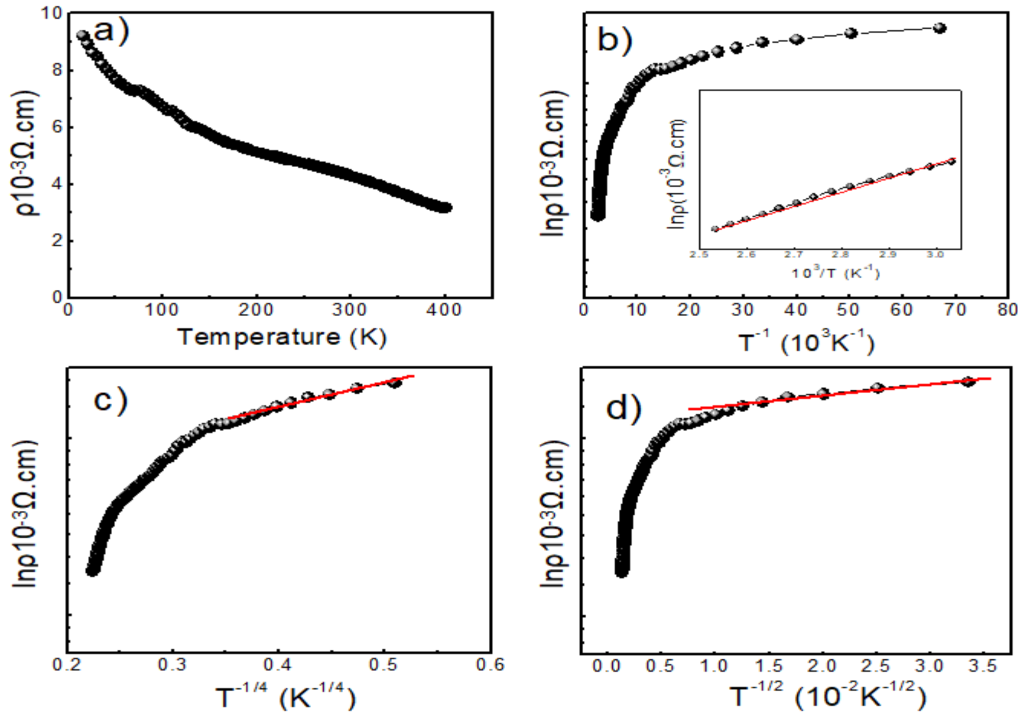

Fig. 3. The temperature dependent of resistivity of $FeAs_2$ film (a), the natural logarithm of electrical resistivity vs. reciprocal temperature (Arrhenius plot) (b), the plot the logarithmic of ρ vs. $T^{-1/4}$, $T^{-1/2}$ (c) and (d), respectively. The inset of Fig. 3 (b) shows linear fitting theory compare to experiment, the variation of the resistivity from 330 to 400 K.

A variation of the resistivity of $FeAs_2$ film vs. temperature is given in Fig. 3 (a). The increase of the resistivity with decrease of the temperature presents a semiconductor behavior in the film. The explanation about conduction mechanism in polycrystalline materials, especially semiconductor, is much complicated. In this work, to better understand the mechanism of conduction of film, we use Arrhenius equation: $\rho = \rho_0 \exp(\Delta/k_B T)$ [8], where ρ_0 is a preexponential factor, Δ is the activation energy, and k_B is the Boltzmann constant. A natural logarithm of electrical resistivity vs. reciprocal temperature (Arrhenius plot) is shown in Fig. 3 (b). In the range of temperature from 330 to 400 K, the variation of the resistivity vs. (1000/T) is like-linear inset in Fig. 3 (b). The electrical activation energy is estimated about 0.20 eV, these results suggest that the mechanism of conduction such as thermionic emission. This mechanism was also reported on polycrystalline CdTe, and GaSe, FeS_2 films before [9-11]. While at low

temperature, the electrical conduction is provided by the so-called variable-range hopping (VRH), that can be expressed by formula: $\rho = \rho_0 \exp[(\Delta/k_B T)^{\beta}]$ [8], where β is determined by the shape of energy-dependent distribution of impurity (DOI) atoms. For β = 1/4 corresponding to the Mott VRH regime, β = 2 corresponding to the Efros and Schklovskii (ES) VRH regime. Fig. 3 (c) and Fig. 3 (d) present the logarithmic plot of ρ vs. $T^{-1/4}$, $T^{-1/2}$ for Mott's and ES VRH, respectively. Using linear fitting function on both cases in range of temperature below 60 K, we conclude that the mechanism of conduction is described as variable range hopping cause of imperfection associated in the film.

Fig. 4 (a) shows negative magnetoresistances at 20 K caused from hopping conduction mechanism at low temperature. The result is quite similar to polycrystalline β-$FeSi_2$ film and n-type InP semiconductor [12-13]. The negative MR is plotted versus $H^{1/2}$, and using fitting function in Fig. 4 (b), it is identified that $H^{1/2}$ dependence of negative magnetoresistance is linear. The result from hopping conduction under applied magnetic field. This behavior is consistent with theoretical predictions and experiments [14-18].

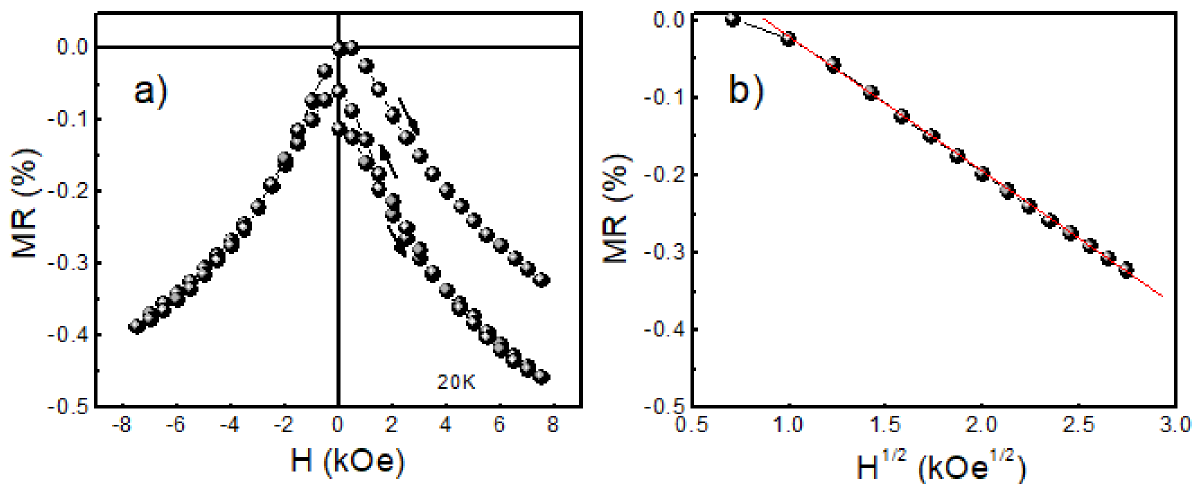

Fig. 4. Magnetoresistance vs. magnetic field at 20 K (a), the negative MR is plotted versus $H^{1/2}$ (b)

The Seebeck coefficient (S) value of the film is negative, indicating electron is dominant charge carriers in the whole temperature range as showed in Fig. 5(a). The temperature dependence of S is expressed by increasing value from 400 to about 300 K. The variation of S value above-below room temperature originates from the change of conduction mechanism. The maximum of S is -138 μV/K at T =300 K, that is smaller than typical bulk sample [3-6]. The temperature dependence of thermoelectric power factor (PF) is shown in Fig. 5 (b). Highest PF value is 4.31 $\mu W/cmK^2$ near room temperature.

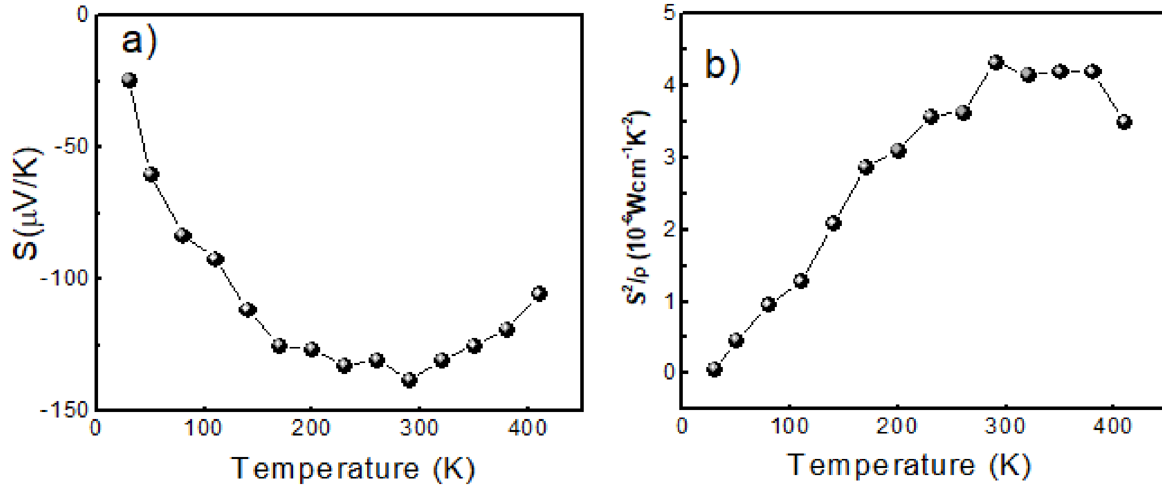

Fig. 5. The temperature dependence of Seebeck coefficient S(T) (a), temperature dependence of thermoelectric power factor (b)

4. CONCLUSIONS

The polycrystalline $FeAs_2$ thin film was grown on a $LaAlO_3$ (100) substrate with orthorhombic phase. The effect of the conduction mechanism to observation of negative magnetoresistance (MR) at low-temperature of 20 K is due to hopping conduction mechanism. The film exhibit semiconductor behavior is found with dominant charge-carrier being electron. Above room temperature, the electrical activation energy is estimated to be 0.20 *eV*, that originates from transport mechanism such as thermionic emission. The maximum of Seebeck coefficient is S = -138 μV/K at T = 300 K that smaller than bulk typical material.

ACKNOWLEDGEMENT

This work was supported by the National Research Foundation of Korea [NRF-2019R1A6A1A11053838, NRF 2020K1A4A7A02095438, and NRF-2022R1A2C1091734]

NOMENCLATURE

S	:	Seebeck coefficient (μV/K)
PF	:	Power factor (μW/cmK^2)
MR	:	Magnetoresistance (%)
ρ	:	Electrical resistivity (Ω.cm)
T	:	Absolute temperature (K)

REFERENCES

[1]. H. Alam, S. Ramakrishna, 2013. A review on the enhancement of figure of merit from bulk to nano-thermoelectric materials. *Nano Energy*, 2 (2), 190–212

[2]. G. D. Mahan, 1997. Good Thermoelectrics, Solid State Physics, 51, 81.

[3]. A. K. L. Fan, G. H. Rosenthal, H. L. Mackinzie and A. Wold, 1972. Preparation and properties of $FeAs_2$ and $FeSb_2$. *Journal of Solid State Chemistry,* 5 (1), 136-143.

[4]. Jan M. Tomczak, K. Haule, T. Miyake, A. Georges, and G. Kotliar, 2010. Thermopower of correlated semiconductors: Application to $FeAs_2$ and $FeSb_2$. *Physical Review B,* 82 (8), 085104

[5]. P. Sun, N. Oeschler, S. Johnsen, B. Iversen, F. Steglich, 2009. Huge Thermoelectric Power Factor: $FeSb_2$ versus $FeAs_2$ and $RuSb_2$. *Applied Physics Express,* 2 (9), 091102.

[6]. H. Usui, K. Suzuki, K. Kuroki, S. Nakano, K. Kudo, and M. Nohara, 2013. Large Seebeck effect in electron-doped $FeAs_2$ driven by a quasi-one-dimensional pudding-mold-type band. *Physical Review B,* 88 (7), 075140.

[7]. H. Usui, K. Suzuki, K. Kuroki, S. Nakano, K. Kudo, and M. Nohara, 2014. Pudding-Mold-Type Band as an Origin of the Large Seebeck Coefficient Coexisting with Metallic Conductivity in Carrier-Doped $FeAs_2$ and $PtSe_2$. *Journal of Electronic Materials*, 43, 1656–1661

[8]. C. Michel, S. D. Baranovskii, P. J. Klar, and P. Thomas, 2006. Strong non-Arrhenius temperature dependence of the resistivity in the regime of traditional band transport. *Applied Physics Letters*, 89(11), 112116.

[9]. A.V. Sukach, V.V. Tetyorkin and N.M. Krolevec, 2010. Mechanisms of carrier transport in CdTe polycrystalline films. *Semiconductor Physics, Quantum Electronics & Optoelectronics*, 13(2), 221-225.

[10]. M. Thamilselvan, K. Premnazeer, D. Mangalaraj, Sa.K. Narayandass, 2003. Field and temperature-dependent electronic transport parameters of amorphous and polycrystalline GaSe thin films. *Physica B: Condensed Matter*, 337(1-4), 404–412.

[11]. B. Ouertani, J. Ouerfelli, M. Saadouna, B. Bessais, H. Ezzaouia, J.C. Berne`de, 2005. Characterization of FeS_2 -pyrite thin films synthesized by sulphuration of amorphous iron oxide films pre-deposited by spray pyrolysis. *Materials Characterization*, 54, 431– 437.

[12]. C. H. Olk, S. M. Yalisove, J. P. Heremans, and G. L. Doll, 1995. Negative magnetoresistance as a result of hopping conduction in polycrystalline thin films of β-$FeSi_2$, *Physical Review B,* 52(7), 4643

[13]. R. Abdia, A. El Kaaouachi , A. Nafidi, G. Biskupski, J. Hemine, 2009. Variable range hopping conductivity and negative magnetoresistance in n-type InP semiconductor, *Solid-State Electronics,* 53(5), 469-472.

[14]. E.Medina and M. Kardar, 1992. Quantum interference effects for strongly localized electrons, *Physical Review B,* 46(16), 9984

[15]. Z. Ovadyahu, 1986. Anisotropic magnetoresistance in a Fermi glass, *Physical Review B,* 33(9), 6552

[16]. A. Kawabata, 1980. Theory of Negative Magnetoresistance I. Application to Heavily Doped Semiconductors, *Journal of the Physical Society of Japan*, 49, 628

[17]. A. Kawabata, 1980. Theory of negative magnetoresistance in three-dimensional systems, *Solid State Communications*, 34(6), 431-432

[18]. R. Rentzsch, K. J. Friedland, and A. N. Ionov, 1988. Negative Magnetoresistance of Neutron-Transmutation-Doped Gallium Arsenide at Variable-Range Hopping, *Physica Status Solidi (b)*, 146(1), 199-206.